0026-895X/09/7606-1220–1227$20.00
MOLECULAR PHARMACOLOGY
Vol. 76, No. 6
59030/3536868
Mol Pharmacol 76:1220–1227, 2009
Printed in U.S.A.

Monoacylglycerol Lipase Limits the Duration of Endocannabinoid-Mediated Depolarization-Induced Suppression of Excitation in Autaptic Hippocampal Neurons

Alex Straiker, Sherry Shu-Jung Hu, Jonathan Z. Long, Andy Arnold, Jim Wager-Miller, Benjamin F. Cravatt, and Ken Mackie

Department of Psychological and Brain Sciences, Gill Center for Biomolecular Science, Indiana University, Bloomington, Indiana (A.S., S.S.-J.H., A.A., J.W.-M., B.F.C., K.M.); and Department of Chemical Physiology, the Scripps Research Institute, La Jolla, California (J.Z.L., B.F.C.)

Received July 6, 2009; accepted September 18, 2009

ABSTRACT

Depolarization-induced suppression of excitation (DSE) is a major form of cannabinoid-mediated short-term retrograde neuronal plasticity and is found in numerous brain regions. Autaptically cultured murine hippocampal neurons are an architecturally simple model for the study of cannabinoid signaling, including DSE. The transient nature of DSE—tens of seconds—is probably determined by the regulated hydrolysis of the endocannabinoid 2-arachidonoyl glycerol (2-AG). No less than five candidate enzymes have been considered to serve this role: fatty acid amide hydrolase (FAAH), cyclooxygenase-2 (COX-2), monoacylglycerol lipase (MGL), and α/β-hydrolase domain (ABHD) 6 and 12. We previously found that FAAH and COX-2 do not have a role in determining the duration of autaptic DSE. In the current study, we found that two structurally distinct inhibitors of MGL [*N*-arachidonoyl maleimide and 4-nitrophenyl 4-(dibenzo[*d*][1,3]dioxol-5-yl(hydroxy)methyl)piperidine-1-carboxylate (JZL184)] prolong DSE in autaptic hippocampal neurons, whereas inhibition of ABHD6 by *N*-methyl-*N*-[[3-(4-pyridinyl)phenyl]methyl]-4′-(aminocarbonyl)[1,1′-biphenyl]-4-yl ester, carbamic acid (WWL70) had no effect. In addition, we developed antibodies against MGL and ABHD6 and determined their expression in autaptic cultures. MGL is chiefly expressed at presynaptic terminals, optimally positioned to break down 2-AG that has engaged presynaptic CB_1 receptors. ABHD6 is expressed in two distinct locations on autaptic islands, including a prominent localization in some dendrites. In summary, we provide strong pharmacological and anatomical evidence that MGL regulates DSE in autaptic hippocampal neurons and, taken together with other studies, emphasizes that endocannabinoid signaling is terminated in temporally diverse ways.

The cannabinoid signaling system functions throughout much of the central nervous system. This system consists of cannabinoid receptors [CB_1 and CB_2 (Matsuda et al., 1990; Munro et al., 1993)], endogenous cannabinoids (endocannabinoids, eCBs) (Devane et al., 1992; Stella et al., 1997), and an assortment of proteins to produce, transport, and break down endocannabinoids. This system is engaged by exogenous cannabinoids, such as the psychoactive ingredients of marijuana and hashish (Gaoni and Mechoulam, 1964). Cannabinoids have been shown to modulate neurotransmission; one form that this modulation takes is depolarization-induced sup-

This work was supported by the National Institutes of Health National Institute on Drug Abuse [Grants DA11322, DA021696, DA024122]; the Lilly Endowment, Inc.; and the Indiana University Light Microscopy Imaging Center.

Article, publication date, and citation information can be found at http://molpharm.aspetjournals.org.

doi:10.1124/mol.109.059030.

ABBREVIATIONS: eCB, endocannabinoid; DSE, depolarization-induced suppression of excitation; DSI, depolarization-induced suppression of inhibition; 2-AG, 2-arachidonoyl glycerol; DAG, diacylglycerol; FAAH, fatty acid amide hydrolase; COX-2, cyclooxygenase 2; MGL, monoacylglycerol lipase; DSI, depolarization-induced suppression of inhibition; URB754, 6-methyl-2-[(4-methylphenyl)amino]-1-benzoxazin-4-one; URB602, [1,1′-biphenyl]-3-yl-carbamic acid, cyclohexyl ester; EPSC, excitatory postsynaptic current; HEK, human embryonic kidney; GST, glutathione transferase; mMGL, mouse MGL; mABHD6, mouse ABHD6; HA, hemagglutinin; rMGL, rat MGL; PB, phosphate buffer; PBS, phosphate-buffered saline; FITC, fluorescein isothiocyanate; DAPI, 4,6-diamidino-2-phenylindole; NAM, *N*-arachidonoyl maleimide; JZL184, 4-nitrophenyl 4-(dibenzo[d][1,3]dioxol-5-yl(hydroxy)methyl)piperidine-1-carboxylate; WWL70, *N*-methyl-*N*-[[3-(4-pyridinyl)phenyl]methyl]-4′-(aminocarbonyl)[1,1′-biphenyl]-4-yl ester, carbamic acid; SR141716, *N*-(piperidin-1-yl)-5-(4-chlorophenyl)-1-(2,4-dichlorophenyl)-4-methyl-1*H*-pyrazole-3-carboxamide hydrochloride; WIN55212-2, (*R*)-(+)-[2,3-dihydro-5-methyl-3-(4-morpholinylmethyl) pyrrolo-[1,2,3-*d*,*e*]-1,4-benzoxazin-6-yl]-1-naphthalenyl-methanone;; WIN, WIN55212-2; SV2, synaptic vesicle protein 2; MAP2, microtubule-associated protein 2.

pression of excitation or inhibition (DSE/DSI) (Kreitzer and Regehr, 2001b; Wilson and Nicoll, 2001). This retrograde inhibition is observed in many regions of the central nervous system (Trettel and Levine, 2003; Yanovsky et al., 2003; Melis et al., 2004; Di et al., 2005). We have previously described DSE in autaptically cultured hippocampal neurons (Straiker and Mackie, 2005). In autaptic neurons, as a result of growth on a limited permissive substrate, neurons synapse (or "autapse") onto themselves, forming an architecturally simple model of synaptic transmission (Bekkers and Stevens, 1991). These neurons exhibit not only robust DSE but also metabotropic suppression of excitation, a corollary of DSE (Straiker and Mackie, 2007) and a form of long-term depression (Kellogg et al., 2009)). The presence of functional DSE in these neurons is possible because these neurons express CB_1 receptors and the machinery to produce and degrade endocannabinoids. We have offered substantial evidence that of the primary candidate endocannabinoids, 2-arachidonoyl glycerol (2-AG) (Stella et al., 1997) and arachidonoyl ethanolamide (anandamide) (Devane et al., 1992), 2-AG is most likely to mediate autaptic DSE (Straiker and Mackie, 2005). For example, inhibition of DAG lipase α, the major synthetic enzyme producing 2-AG (Bisogno et al., 2003), prevents DSE (Straiker and Mackie, 2005). In addition, although brief arachidonoyl ethanolamide application inhibits excitatory postsynaptic currents, this inhibition does not recover even over the course of ~10 min. This contrasts to inhibition by brief 2-AG application, which recovers with a time course that closely mimics that of DSE. Thus, the identity of the receptor and eCB underlying autaptic DSE are known, but how 2-AG signaling in autaptic DSE is terminated remains elusive. To date, no less than five enzymes have received serious attention as possible mediators of 2-AG hydrolysis. Fatty acid amide hydrolase (FAAH) can break down 2-AG, as can cyclooxygenase 2 (COX-2) (Cravatt et al., 1996; Kozak et al., 2000, 2004). Inhibition of the latter has been shown to prolong the time course of DSI recovery in hippocampal slices (Kim and Alger, 2004) and in cultured neurons (Hashimotodani et al., 2007; Straiker and Mackie, 2009). However, we have previously tested inhibitors for both of these enzymes and found no effect on DSE in autaptic hippocampal neurons (Straiker and Mackie, 2005). The enzyme that accounts for the majority of 2-AG breakdown in brain homogenates is monoacylglycerol lipase (MGL) (Blankman et al., 2007). Anatomical studies have established the presence of MGL in presynaptic terminals, making it well sited to break down 2-AG after DSE/DSI (Dinh et al., 2002; Gulyas et al., 2004). Furthermore, MGL has been implicated in regulation of retrograde eCB signaling, but with the use of nonspecific inhibitors, such as 1) methyl arachidonoyl fluorophosphonate (Hashimotodani et al., 2007), which acts on FAAH (De Petrocellis et al., 1997; Deutsch et al., 1997), phospholipase A_2 (Lio et al., 1996), and CB_1 (Fernando and Pertwee, 1997); 2) the known FAAH inhibitor arachidonoyltrifluoromethane (Koutek et al., 1994; Hashimotodani et al., 2007); 3) the drug URB754 (Makara et al., 2005), the usefulness of which has since been called into question (Saario et al., 2006; Hashimotodani et al., 2007); or 4) URB602 (Makara et al., 2005), a relatively weak blocker (King et al., 2007) with variable and limited efficacy (Saario et al., 2006) but one that we have nonetheless tested. The attention that has been given to the subject underscores its importance, but only recently have clearly selective and potent inhibitors been described for MGL (Long et al., 2009). Complicating the picture, two more enzymes have now been shown to hydrolyze 2-AG. ABHD6 and ABHD12 each account for a portion of 2-AG hydrolysis in brain homogenates (Blankman et al., 2007). Although ABHD6 and ABHD12 represent only a relatively small fraction of the total 2-AG hydrolysis in brain homogenates, their existence raises an important question—which enzyme breaks down 2-AG for a given population of cells? Depending on the subcellular localization of these enzymes, it remains possible that an enzyme of relatively low abundance as measured in a homogenate assay terminates DSE in a specific set of synapses, particularly if it is localized to the site of 2-AG action. An enzyme's relative contribution may vary among neuronal populations and within a given neuron; it may even be shared in some manner, as it appears to be in one form of autaptic DSI (Straiker and Mackie, 2009) and other forms of hippocampal DSI (Kim and Alger, 2004; Hashimotodani et al., 2007). To explore this question, we used an assortment of enzyme inhibitors and antibodies developed to detect these proteins to assess their roles in mediating breakdown of 2-AG to terminate DSE in autaptic hippocampal neurons.

Materials and Methods

Culture Preparation. All procedures used in this study were approved by the Animal Care Committee of the Indiana University and conform to the recommendations of the *Guide for the Care and Use of Laboratory Animals* (Institute of Laboratory Animal Resources, 1996). Mouse (CD1 strain) hippocampal neurons isolated from the CA1-CA3 region were cultured on microislands as described previously (Furshpan et al., 1976; Bekkers and Stevens, 1991). Neurons were obtained from animals (age postnatal day 0–2) and plated onto a feeder layer of hippocampal astrocytes that had been laid down previously (Levison and McCarthy, 1991). Cultures were grown in high-glucose (20 mM) medium containing 10% horse serum without mitotic inhibitors and used for recordings after 8 days in culture and for no more than 3 h after removal from culture medium.

Electrophysiology. When a single neuron is grown on a small island of permissive substrate, it forms synapses—or "autapses"—onto itself. All experiments were performed on isolated autaptic neurons. Whole-cell voltage-clamp recordings from autaptic neurons were carried out at room temperature using Axopatch 200A amplifier (Molecular Devices, Sunnyvale, CA). The extracellular solution contained 119 mM NaCl, 5 mM KCl, 2.5 mM $CaCl_2$, 1.5 mM $MgCl_2$, 30 mM glucose, and 20 mM HEPES. Continuous flow of solution through the bath chamber (~2 ml/min) ensured rapid drug application and clearance. Drugs were typically prepared as stock, then diluted into extracellular solution at their final concentration and used on the same day.

Recording pipettes of 1.8 to 3 MΩ were filled with 121.5 mM potassium gluconate, 17.5 mM KCl, 9 mM NaCl, 1 mM $MgCl_2$, 10 mM HEPES, 0.2 mM EGTA, 2 mM MgATP, and 0.5 mM LiGTP. Access resistance and holding current were monitored, and only cells with both stable access resistance and holding current were included for data analysis. Conventional stimulus protocol: the membrane potential was held at −70 mV and excitatory postsynaptic currents (EPSCs) were evoked every 20 s by triggering an unclamped action current with a 1.0-ms depolarizing step. The resultant evoked waveform consisted of a brief stimulus artifact and a large downward spike representing inward sodium currents, followed by the slower excitatory postsynaptic current. The size of the recorded EPSCs was calculated by integrating the evoked current to yield a charge value (in picocoulombs). Calculating the charge value in this manner yields an indirect measure of the amount of neurotransmitter released while minimizing the effects of cable distortion on currents gener-

ated far from the site of the recording electrode (the soma). Data were acquired at a sampling rate of 5 kHz.

DSE Stimuli. After establishing a 10- to 20-s 0.5-Hz baseline, DSE was evoked by depolarizing to 0 mV for 1 to 10 s, followed by resumption of a 0.5-Hz stimulus protocol for 10 to ≥80 s, until EPSCs recovered to baseline values.

Human Embryonic Kidney Cell Cultures. Human embryonic kidney (HEK) cells were purchased from the American Type Culture Collection (Manassas, VA). Dulbecco's modified Eagle's medium, penicillin, streptomycin, and fetal bovine serum (FBS) were purchased from Invitrogen (Carlsbad, CA). HEK cells were grown in Dulbecco's modified Eagle's medium with 10% FBS, 100 units/ml penicillin, and 100 μg/ml streptomycin at 37°C in 5% CO_2 humidified air.

Antibody Generation. A GST fusion protein expression construct was produced by inserting the DNA coding for a 35-amino acid peptide (PNMTLGRIDSSVLSRNKSEVDLYNSDPLVCRAGLK) from mouse MGL (mMGL) or a 38-amino acid peptide (DMPGHEGTTRSSLDDLSIVGQVKRIHQFVECLKLNKKP) from mouse ABHD6 (mABHD6) into the pGEX-3X vector at BamHI and EcoRI restriction sites. Each fusion protein was purified from BL21 *Escherichia coli* lysates on a glutathione Sepharose column and was injected into two rabbits to generate antisera (Cocalico Biologicals, Inc., Reamstown, PA) using standard approaches (Bodor et al., 2005). The antiserum was purified in two steps, first by removal of GST antibodies with a GST column and then by binding to and elution from an affinity column made with the injected GST fusion protein.

Fluorescent Immunocytochemistry of HEK Cells Transiently Expressing V5-rMGL or HA-mABHD6. HEK cells growing on glass coverslips were transiently transfected with either V5-tagged rat MGL (rMGL) or HA-tagged mABHD6. The following day they were washed three times with ice-cold 0.1 M phosphate buffer (PB) and then fixed with 4% paraformaldehyde in PB for 20 min at room temperature. Cells were then washed twice with PB and three times with 150 mM NaCl + PB (0.1 M PBS). Next, cells were incubated with a blocking solution (5% donkey serum + 0.1% saponin in 0.1 M PBS) for 30 min at room temperature. Cells transiently transfected with V5-rMGL were incubated with affinity-purified mMGL antibody (diluted 1:2000 in the blocking solution) and anti-V5 antibody (1:500; Invitrogen), and cells transiently transfected with HA-mABHD6 were incubated with affinity-purified mABHD6 antibody (diluted 1:2000 in the blocking solution) and anti-HA antibody for 3 h at room temperature and then washed six times with 0.1 M PBS. Cells were next incubated with fluorescein isothiocyanate (FITC)-conjugated donkey anti-rabbit secondary antibody (1:150; Jackson ImmunoResearch Laboratories, Inc., West Grove, PA) and Texas Red-conjugated donkey anti-mouse secondary antibody (1:150) for 1 h at room temperature. Finally, cells were washed three times with 0.1 M PBS, twice with 0.1 M PB, and three times with water and air-dried. Dried coverslips were inverted and mounted on a drop of Vectashield containing DAPI (Vector Laboratories, Inc., Burlingame, CA). Stained cells were examined with a Nikon Eclipse (TE2000-E) confocal microscope (Nikon, Tokyo, Japan) with the appropriate excitation filters for FITC (MGL or ABHD6) and Texas Red (V5 or HA). All figures are representative of at least three experiments with at least three fields of view analyzed per experiment.

Drugs were purchased from Tocris Cookson (Ellisville, MO), Cayman Chemical (Ann Arbor, MI), or Sigma-Aldrich (St. Louis, MO). rMGL with a V5 epitope (rMGL-V5) was the kind gift of Dr. Daniele Piomelli (University of California, Irvine, CA).

Staining of Autaptic Cultures. Coverslips with autaptic cultured neurons (8–15 days) were fixed and washed as above. Cells were incubated with a neuron blocking solution (5% milk in 0.1 M PBS + 0.3% Triton-X) for 30 min at room temperature. Neurons were incubated with antibodies against MGL (1:400), ABHD6 (1:1000), or CB_1 (1:500–1000) on their own or coincubated with antibodies against marker proteins [SV2 (1:2000; Developmental Studies Hybridoma Bank, University of Iowa, Iowa City, IA), a marker for synaptic vesicles; 2H3 (1:600; Developmental Studies Hybridoma Bank, University of Iowa), an axonal marker; MAP2 (1:1000; Cell Signaling Technology, Danvers, MA), a dendritic marker; and glutamine synthetase (1:200; Millipore, Billerica, MA), a glial marker] overnight at 4°C and then washed six times with 0.1 M PBS. Cells were next incubated with FITC-conjugated donkey secondary antibody [anti-rabbit or anti-mouse (1:200, Jackson ImmunoResearch Laboratories, Inc., West Grove, PA) or Texas Red-conjugated donkey secondary antibody (1:200; anti-rabbit or anti-mouse)] for 1.5 h at room temperature. Finally, coverslips were washed, dried, and mounted as described above. Images were acquired with a confocal microscope (TCS SP5; Leica Microsystems, Wetzlar, Germany) using Leica LAS AF software and a 63× oil objective. Images were processed using ImageJ (http://rsbweb.nih.gov/ij/) and/or Photoshop (Adobe Systems Inc., Mountain View, CA). Images were modified only in terms of brightness and contrast.

Results

To investigate which enzyme is most likely to mediate breakdown of 2-AG in autaptic hippocampal neurons, we took two approaches: electrophysiological and immunohistochemical. We examined inhibitors of two enzymes hypothesized to break down 2-AG in terms of their ability to slow the decay of DSE, and we developed antibodies against these enzymes to assess their cellular localization.

The study of eCB breakdown has been made more challenging by the number of candidates (currently five) and the scarcity of selective inhibitors. It was the existence of reliable inhibitors for FAAH and for COX-2 that allowed us assemble evidence against a role of these enzymes in autaptic DSE (Straiker and Mackie, 2005). In the case of MGL, the action of URB754, an early promising inhibitor, was found to be artifactual (Makara et al., 2005; Saario et al., 2006). URB602 (100 μM) was reported to be modestly effective (Makara et al., 2005) but has also been found ineffectual (Connell et al., 2005; Saario et al., 2006). And as mentioned above, methyl arachidonoyl fluorophosphonate and arachidonoyltrifluoromethane (Hashimotodani et al., 2007) are believed to inhibit other endocannabinoid-metabolizing enzymes (Lio et al., 1996; De Petrocellis et al., 1997; Deutsch et al., 1997; Fernando and Pertwee, 1997). Two new MGL inhibitors have recently been identified: *N*-arachidonoyl maleimide (NAM) and JZL184 (Saario et al., 2005; Long et al., 2009). In addition, WWL70 seems to be a selective inhibitor of ABHD6 (Li et al., 2007). However, no selective inhibitor is known for ABHD12. Consequently, we examined whether inhibition of MGL or ABDH6 prolonged the duration of DSE.

First we tested NAM. Using whole-cell patch recording of autaptic hippocampal neurons, we elicited a baseline DSE in an autaptic neuron by depolarizing the cell for 3 s. Recordings were maintained while neurons were treated with NAM for 10 min, followed by DSE elicited in the presence of the drug. We found that after exposure to 10 μM NAM in this manner, DSE recovery was prolonged: half-life for recovery ($t_{1/2}$), or the time it takes to reach 50% recovery, almost doubled after 10 min of NAM treatment [Fig. 1A, $t_{1/2}$ recovery time course: control, 43 s (95% confidence interval, 40–46 s); 10 μM NAM, 81 s (95% confidence interval, 71–96 s), $n = 5$]. This experiment provides the first evidence that MGL has a role in eCB breakdown in autaptic hippocampal neurons. However, to verify this result, we tested a structurally dis-

tinct, highly potent, and very selective inhibitor, JZL184 (Long et al., 2009). We found that a 10-min treatment with 100 nM JZL184 produced a pronounced prolongation of DSE recovery [Fig. 1B, $t_{1/2}$ recovery time course: control, 38 s (95% confidence interval, 33–46 s); 100 nM JZL184, 117 s (95% confidence interval, 90–167 s), $n = 6$]. JZL184 on its own decreased EPSCs only in neurons with strong DSE (<5% of neurons, data not shown) consistent with our results for DSI (Straiker and Mackie, 2009). These neurons (<5% of those tested) were excluded from study. It is noteworthy that in the few cases we tested, JZL184 inhibition was reversed by CB_1 antagonist SR141716 (100 nM), and we found that SR141716 fully reversed inhibition (data not shown). If JZL184 action occurs via MGL, one would expect a JZL184 effect on bath-applied 2-AG inhibition but not on inhibition by a synthetic agonist such as WIN55212-2 (WIN). As a further test of MGL specificity, in same-cell experiments, we puffed 2-AG (5 μM, 5 s) or WIN (50 nM, 5 s) onto cells before and again after treatment with JZL184 (100 nM, 10 min). We found that the half-life of the 2-AG recovery time course ($t_{1/2}$) was much slower than the control time course after treatment with JZL184 [Fig. 1C, $t_{1/2}$ recovery time course for puffed 2-AG: control, 59 s (95% confidence interval, 40–112 s); 100 nM JZL184, 360 s (95% confidence interval, 259–585 s), $n = 4$]. Because the $t_{1/2}$ recovery time course for WIN is much longer than that for 2-AG [5.5 min versus 41 s (Straiker and Mackie, 2005)], making it impractical to measure changes in the recovery time course, we examined peak inhibition for WIN, using a low concentration of this agonist. We reasoned that if the JZL184-induced prolongation of the 2-AG inhibition were due to an enhancement of CB_1 signaling, then JZL184 would also increase the potency of a submaximal concentration of CB_1 agonist. We therefore used a brief puff of 50 nM WIN, resulting in an inhibition of ~20%, well below the ~50% generally seen for maximal inhibition with bath applied WIN. The use of a low concentration of WIN also helps avoid problems with the known nonselectivity of WIN at higher concentrations [i.e., >1 μM (Shen and Thayer, 1998)] A second puff of WIN in the same cells after treatment with JZL184 resulted in no greater inhibition [Fig. 1D, relative EPSC charge for WIN puff (50 nM, 5 s, control): 0.80 ± 0.04; (JZL 184) 0.82 ± 0.06, $n = 4$, $p > 0.05$ paired t test]. Taken together, these pharmacological experiments provide strong evidence that MGL is the major enzyme that hydrolyzes 2-AG during autaptic DSE and thereby determines the duration of DSE.

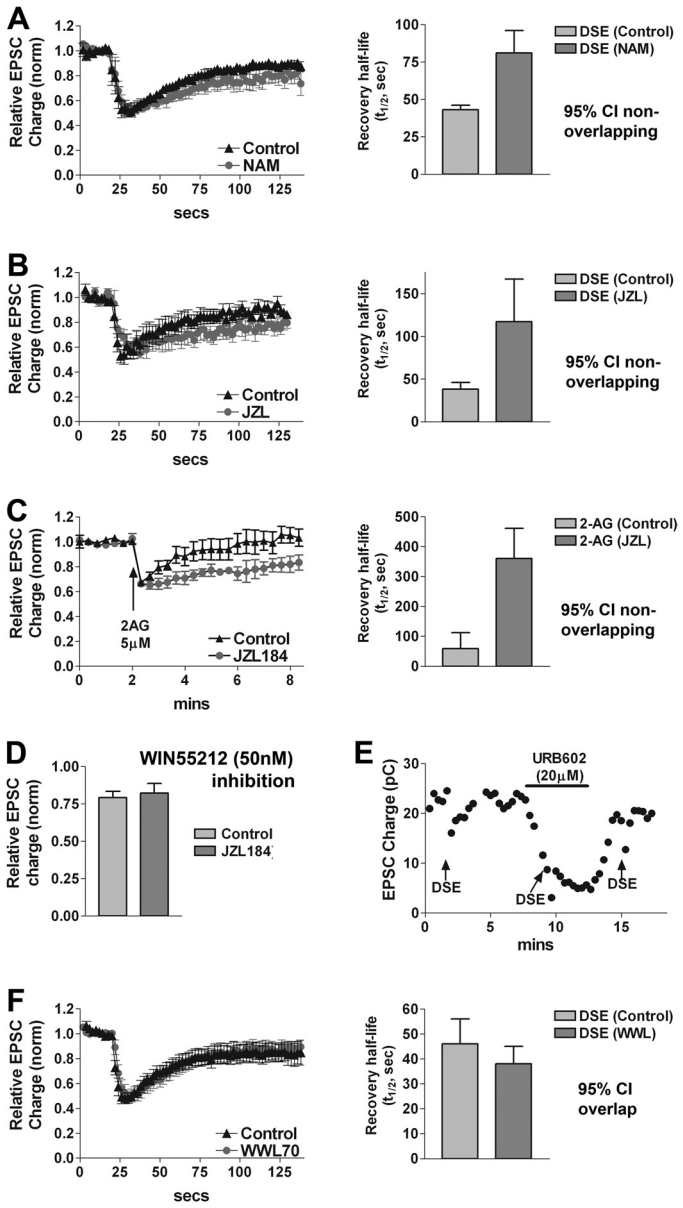

Fig. 1. MGL inhibition prolongs DSE duration. A, time course of DSE in cells before (black triangles) and after (gray circles) treatment with a MGL inhibitor NAM (10 μM, 10 min). Right, bar graph illustrates $t_{1/2}$ recovery half-life time courses for A. B, time course of DSE in cells before (black triangles) and after (gray circles) treatment with a selective MGL inhibitor JZL184 (100 nM, 10 min). Right, bar graph illustrates $t_{1/2}$ recovery half-life time courses for B. C, time course in response to puffed 2AG (5 μM, 5 s) before (black triangles) and after (gray circles) treatment with JZL184 (100 nM, 10 min). Right, bar graph illustrates $t_{1/2}$ recovery half-life time courses for C. D, bar graphs show relative EPSC charge after puffed CB1 agonist WIN (50 nM, 5 s) before or after treatment with JZL184 (100 nM, 10 min). E, sample EPSC time course shows that putative MGL inhibitor URB602 (20 μM) directly and reversibly inhibits EPSCs. F, the ABHD6 inhibitor WWL70 (10 μM, 10 min) has no effect on recovery time course of DSE. Right, bar graph illustrates $t_{1/2}$ recovery half-life time courses for F. Error bars are 95% CI except D, which shows S.E.M..

Another compound, URB602, has been reported to block MGL activity (Connell et al., 2005). However, we found that at 20 μM, URB602 substantially and rapidly diminished EPSCs (Fig. 1E). In principle, this synaptic inhibition could be due to inhibition of MGL, thereby increasing 2-AG, which activates CB_1 receptors to inhibit EPSCs. To test this hypothesis, we attempted to reverse URB602 inhibition with the CB_1 receptor antagonist SR141716 (100–200 nM, a concentration sufficient to reverse CB_1 activation by 5 μM 2-AG), but without success (data not shown). We conclude that URB602 inhibition of EPSCs occurs via a CB_1- and MGL-independent mechanism. Although potentially interesting, this finding makes URB602 impractical for the study of MGL inhibition in this preparation.

In principle, ABHD6 might still play a role in DSE recovery. If both enzymes were expressed at the presynaptic terminal, they could, in principle, share this role, each responsible for part of the 2-AG breakdown. However, treatment with a high concentration of WWL70 did not slow the DSE recovery time course [Fig. 1F, 10 μM; $t_{1/2}$ recovery time course: control, 46 s (95% confidence interval, 39–56 s); 10 μM WWL70 (10 min), 38 s (95% confidence interval, 33–45

s), $n = 5$]. It is possible that ABHD6 plays a subtle role that is not readily distinguished with our DSE protocols or may play a role in metabolizing 2-AG that is released by different stimulation paradigms. In part for this reason, we explored the cellular expression/localization of these proteins.

MGL and ABHD6 Localization as Determined by Immunocytochemistry. 2-AG engages presynaptic CB_1 receptors to inhibit synaptic transmission in autaptic neurons (Sullivan, 1999; Straiker and Mackie, 2005). The presynaptic terminal therefore represents a likely site of expression for an enzyme acting to break down 2-AG after DSE. In principle, the localization could be postsynaptic, but this would require a second traverse by 2-AG of the synapse before it is degraded. In any event, MGL is expected to be in relatively close proximity to 2-AG's site of action: CB_1 receptors.

The first step was to confirm the presynaptic localization of CB_1 receptors. By costaining with SV2, which labels synaptic vesicles and therefore presynaptic terminals, we verified that CB_1 receptors localize to presynaptic terminals (Fig. 2B) in autaptic neurons. We observed only partial overlap between CB_1 and SV2. There are at least two reasons for this partial overlap: 1) in cultured neurons, CB_1 staining is found not only in presynaptic terminals but also along axons, presumably in transit; and 2) it is possible, even likely, that not all synaptic terminals express CB_1 receptors. For example, different terminals may be at different stages of development or plasticity.

MGL. To determine where MGL and ABHD6 are expressed in autaptic hippocampal neurons, we developed antibodies against these proteins. As shown in Figs. 3 and 4, respectively, these antibodies selectively label HEK293 cells in which MGL and ABHD6 are overexpressed. Transient expression of rMGL with a V5 epitope (rMGL-V5) allowed us to confirm the specificity of our newly developed antibody against MGL. The same procedure was followed for ABHD6 (HA and ABHD6 antibodies). In both cases, overlap was almost complete (Figs. 3, A–D, and 4, A–D).

With evidence for the selectivity of these antibodies in hand, we studied the localization of MGL and ABHD6 in autaptic hippocampal neurons. MGL staining was suggestive of a primarily neuronal localization, observed as large puncta above the astrocyte feeder layer (Fig. 3E). To ascertain whether the staining was in fact neuronal, and more specif-

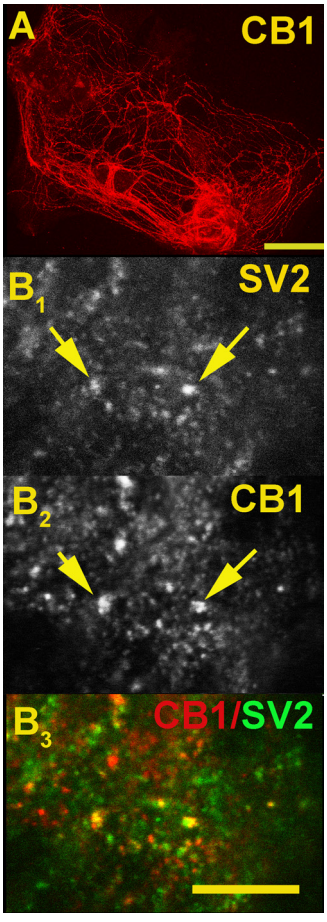

Fig. 2. CB_1 is expressed at presynaptic terminals in autaptic hippocampal neurons. A, micrograph shows CB_1 staining in autaptic hippocampal neurons. Scale bar, 50 μm. B1, synaptic vesicle marker SV2. B2, CB1. Arrows highlight points of overlap. B3, overlay of B1 and B2. Costaining of CB1 (red) with the synaptic vesicle marker SV2 (green) shows (in overlap, yellow) that CB1 is present at presynaptic terminals. Scale bar, 7.5 μm.

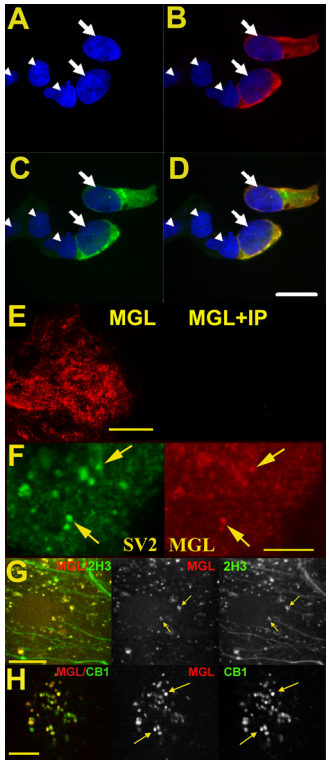

Fig. 3. MGL labels presynaptic terminals. HEK293 cells were transiently transfected with V5-tagged rMGL and stained using V5 (1:500) and MGL (1:2000) antibodies. A, DAPI staining identifies cell nuclei (arrowheads). B, V5 antibody (detected with Texas Red secondary) staining shows two V5-rMGL transfected cells (nuclei indicated by arrows). C, mMGL staining (FITC) labels the same cells identified with the V5 antibody. D, Overlay of V5 and mMGL images shows both antibodies overlap completely, DAPI fluorescence identifies all cells in the field. The nontransfected cells are not labeled with the mMGL antibody. Scale bar, 15 μm. E, left, MGL staining of an autaptic culture; right, staining (taken at same settings) when the MGL antibody was coincubated with immunizing protein (IP, 5 μg/ml). Scale bar, 25 μm. F, separate images from same cell show on the left (green) SV2, a marker for presynaptic terminals, and on the right MGL (red). Arrows identify two of the numerous points of overlap. Scale bar, 10 μm. G, left, MGL (red) and staining for axonal marker 2H3 (green, overlap in yellow). Right, MGL (red) and 2H3 (green) channels, with arrows identifying two points of overlap. Scale bar, 12.5 μm. H, left, MGL (red) and staining for CB1 (green, overlap in yellow). Center, MGL. Right, CB_1, with arrows identifying two points of overlap. Scale bar, 12.5 μm.

ically presynaptic, we costained with SV2, a synaptic vesicle marker. We observed substantial overlap for MGL and SV2 (Fig. 3F, arrows). The overlap was not complete, with some MGL staining free of SV2 and vice versa. However, this indicates that MGL is located at many presynaptic terminals, and therefore well situated to break down 2-AG after activation of CB_1 receptors. MGL staining also partially colocalized with axons stained with the axonal marker 2H3 (Fig. 3G, arrows). Based on these results, one would predict a high degree of colocalization at synaptic terminals for MGL and CB_1. Costaining of MGL with CB_1 yielded substantial overlap at putative synaptic terminals (Fig. 3H, arrows).

ABHD6. Although the ABHD6 inhibitor WWL70 failed to alter the time course of DSE, we found that an antibody developed against ABHD6 did label autaptic islands, with staining restricted to two at least superficially neuron-like compartments, suggesting that ABHD6 is expressed in neuronal cultures (Fig. 4, E1 and E2). One staining pattern was largely restricted to the periphery of a given island, often in a nearly circular pattern. Although this pattern often coincided with the border of the astrocyte feeder layer, this was not always the case. In the example shown in Fig. 4, the labeling was often limited to a single process at or near the edge of a given island, suggestive of neuronal localization (Fig. 4F, inset). However, this staining does not overlap with the presynaptic marker SV2, the axonal marker 2H3 (data not shown), or the dendritic marker MAP2 (data not shown). Nearly every island exhibited this pinwheel labeling, regardless of the presence of synapses (as evidenced by SV2 staining). This ABHD6 staining may in fact be glial in nature. To test this, we costained with glutamine synthetase, a marker for some astrocytes and oligodendrocytes (Norenberg and Martinez-Hernandez, 1979; Fages et al., 1988; Tansey et al., 1991). However, we found that ABHD6 and glutamine synthetase staining were mutually exclusive (Fig. 4, G-H), although this result does not rule out subpopulation-specific astrocyte expression of ABHD6.

The second ABHD6 staining pattern was more explicitly neuronal—limited to putative neuronal processes and puncta above the plane of the astrocyte feeder layer. The presynaptic

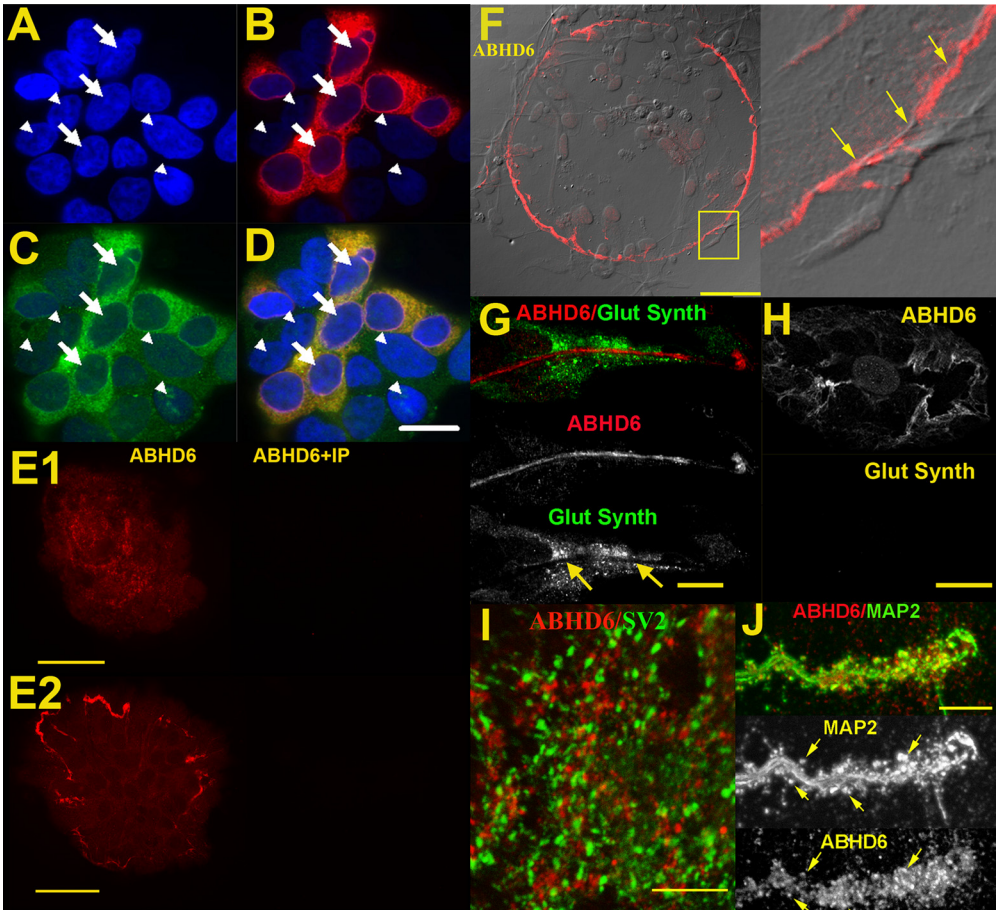

Fig. 4. ABHD6 immunoreactivity in hippocampal neurons. HEK293 cells were transiently transfected with HA-tagged mABHD6 and stained using HA (1:500) and ABHD6 (1:2000) antibodies. A, DAPI staining identifies cell nuclei (arrowheads). B, HA antibody (detected with Texas Red secondary) staining shows HA-mABHD6 transfected cells (nuclei indicated by arrows). C, mABHD6 staining (FITC) labels the same cells identified with the HA antibody. D, Overlay of HA- and mABHD6-images shows both antibodies overlap completely, DAPI fluorescence identifies all cells in the field. The nontransfected cells (which endogenously express ABHD6) are weakly labeled with the mABHD6 antibody. Scale bar, 15 μm. E1 and E2, left, ABHD6 staining of an autaptic culture; right, ABHD6 antibody preincubated with immunizing protein (5 μg/ml) Scale bars, 25 and 50 μm. F, left, circular ABHD6 staining commonly found on autaptic islands. Note that the island (cells visible in differential interference contrast microscopy) extends beyond the edge of the staining. Scale bar, 50 μm. G, ABHD6 (red) and glutamine synthetase (Glut Synth, green) staining are mutually exclusive (arrows). Scale bar, 7.5 μm. H, an example of ABHD6 positive neuronal island with no glia positive for glutamine synthetase. Scale bar, 10 μm. I) ABHD6 (red) does not colocalize with SV2 (green). Scale bar, 7.5 μm. J, ABHD6 (red) does colocalize with some dendritic spines labeled by MAP2 (green, overlap in yellow). Top, overlap; middle and bottom, MAP2 and ABHD6, respectively, with arrows to identify several points of overlap. Scale bar, 7.5 μm.

marker SV2 did not overlap with ABHD6; rather, it was juxtaposed to it (Fig. 4I). MAP2, which labels dendrites, partly overlapped with ABHD6 staining, at what appeared to be dendritic spines and/or terminals (Fig. 4J, arrows). However, there was additional ABHD6 staining that did not overlap with MAP2. In no case did ABHD6 immunoreactivity overlap with staining for 2H3 (data not shown).

Discussion

DSE and DSI are CB_1 cannabinoid receptor- and eCB-mediated forms of transient retrograde inhibition, each lasting for tens of seconds (Kreitzer and Regehr, 2001a,b; Ohno-Shosaku et al., 2001; Wilson and Nicoll, 2001; Wilson et al., 2001). The duration of DSI and DSE are probably determined by a combination of diffusion of 2-AG away from CB_1, uptake, and degradation. In this study, we have addressed the degradation step. Several candidate enzymes have been found to be capable of degrading 2-AG, including FAAH, MGL, COX-2, and, more recently, ABHD6 and ABHD12 (Cravatt et al., 1996; Kozak et al., 2000; Dinh et al., 2002; Kozak et al., 2004; Blankman et al., 2007). Of the first three, MGL is favored (Kim and Alger, 2004; Hashimotodani et al., 2007; Straiker and Mackie, 2009). COX-2 inhibition enhances DSI but has not been found to alter the recovery time course of exogenously applied 2-AG (Kim and Alger, 2004; Hashimotodani et al., 2007). This is consistent with schemes in which either presynaptic COX-2 decrease the DAG pool accessible to DAG lipase or generates oxygenated 2-AG (PGE_2-glycerol ester, which is not a CB_1 agonist). ABHD6 and ABHD12 remain to be investigated systematically.

Definitive identification of the responsible enzyme for terminating eCB-plasticity has remained elusive largely for lack of sufficiently efficacious and selective pharmacological inhibitors. The recent development of new inhibitors for MGL and ABHD6 offer an opportunity to revisit the question of DSE termination. Taken together with our previous work on this subject (Straiker and Mackie, 2005), our results provide anatomical and functional evidence that strongly favors a role for MGL over ABHD6, COX-2, or FAAH in termination of autaptic DSE. MGL is present presynaptically and is therefore well positioned to break down 2-AG after commencement of DSE. Two structurally distinct MGL inhibitors each slow the DSE recovery time course, whereas JZL184 slows that for exogenously applied 2-AG. In contrast, ABHD6 is not present presynaptically in autaptic neurons and the ABHD6 inhibitor, WWL70, has no effect on the autaptic DSE time course.

Our electrophysiological and immunohistochemical results argue against a role for ABHD6 in terminating autaptic DSE. Although the protein is not ideally situated to influence DSE recovery in these neurons, the presence of a posts-synaptic enzyme capable of hydrolyzing 2-AG raises interesting possibilities. In principle, such an enzyme could be involved in regulating nonsynaptic 2-AG levels, in limiting postsynaptic spillover, in regulating other forms of eCB-mediated plasticity, or even in determining a set-point for 2-AG production.

The presence of two distinct forms of autaptic DSI and one form of autaptic DSE in populations of cultured hippocampal neurons grown under otherwise identical conditions invites a dissection of the differences between these forms of retrograde inhibition. In brief, the prominent forms of autaptic DSI come in a fast form (autaptic DSI_{FAST}) regulated by both MGL and COX-2 and a slow form (autaptic DSI_{SLOW}) regulated by MGL but not COX-2 (Straiker and Mackie, 2009). These forms of autaptic DSI both have a much lower ED_{50} (i.e., less duration of depolarization is required to reach 50% inhibition) than autaptic DSE but an identical EC_{50} for 2-AG inhibition of synaptic transmission, suggesting that the inhibitory neurons have a greater ability to produce 2-AG. It is intriguing that autaptic DSE and autaptic DSI_{SLOW} coincide in terms of both their recovery time courses and the enzyme (MGL) found to terminate DSE/DSI, whereas the faster autaptic DSI_{FAST} is regulated by two enzymes. This ability to "tune" the duration of endocannabinoid-mediated plasticity by differential expression of degrading enzymes may prove to be a more general mechanism for termination of DSE, DSI, and other forms of endocannabinoid-mediated plasticity.

Summary. Making use of autaptically cultured murine hippocampal neurons, an architecturally simple culture model of cannabinoid signaling, we have found clear pharmacological and immunocytochemical evidence for a role of MGL in terminating autaptic DSE. Taken together with our work in inhibitory autaptic neurons, our results present a model for control of termination of DSE/DSI whereby faster breakdown is achieved via differential expression of 2-AG hydrolyzing enzymes.

References

Bekkers JM and Stevens CF (1991) Excitatory and inhibitory autaptic currents in isolated hippocampal neurons maintained in cell culture. *Proc Natl Acad Sci U S A* **88:**7834–7838.

Bisogno T, Howell F, Williams G, Minassi A, Cascio MG, Ligresti A, Matias I, Schiano-Moriello A, Paul P, Williams EJ, et al. (2003) Cloning of the first sn1-DAG lipases points to the spatial and temporal regulation of endocannabinoid signaling in the brain. *J Cell Biol* **163:**463–468.

Blankman JL, Simon GM, and Cravatt BF (2007) A comprehensive profile of brain enzymes that hydrolyze the endocannabinoid 2-arachidonoylglycerol. *Chem Biol* **14:**1347–1356.

Bodor AL, Katona I, Nyíri G, Mackie K, Ledent C, Hájos N, and Freund TF (2005) Endocannabinoid signaling in rat somatosensory cortex: laminar differences and involvement of specific interneuron types. *J Neurosci* **25:**6845–6856.

Connell K, Bolton N, Olsen D, Piomelli D, and Hohmann AG (2005) Role of the basolateral nucleus of the amygdala in endocannabinoid-mediated stress-induced analgesia. *Neurosci Lett* **397:**180–184.

Cravatt BF, Giang DK, Mayfield SP, Boger DL, Lerner RA, and Gilula NB (1996) Molecular characterization of an enzyme that degrades neuromodulatory fatty-acid amides. *Nature* **384:**83–87.

De Petrocellis L, Melck D, Ueda N, Maurelli S, Kurahashi Y, Yamamoto S, Marino G, and Di Marzo V (1997) Novel inhibitors of brain, neuronal, and basophilic anandamide amidohydrolase. *Biochem Biophys Res Commun* **231:**82–88.

Deutsch DG, Omeir R, Arreaza G, Salehani D, Prestwich GD, Huang Z, and Howlett A (1997) Methyl arachidonyl fluorophosphonate: a potent irreversible inhibitor of anandamide amidase. *Biochem Pharmacol* **53:**255–260.

Devane WA, Hanus L, Breuer A, Pertwee RG, Stevenson LA, Griffin G, Gibson D, Mandelbaum A, Etinger A, and Mechoulam R (1992) Isolation and structure of a brain constituent that binds to the cannabinoid receptor. *Science* **258:**1946–1949.

Di S, Boudaba C, Popescu IR, Weng FJ, Harris C, Marcheselli VL, Bazan NG, and Tasker JG (2005) Activity-dependent release and actions of endocannabinoids in the rat hypothalamic supraoptic nucleus. *J Physiol* **569:**751–760.

Dinh TP, Carpenter D, Leslie FM, Freund TF, Katona I, Sensi SL, Kathuria S, and Piomelli D (2002) Brain monoglyceride lipase participating in endocannabinoid inactivation. *Proc Natl Acad Sci U S A* **99:**10819–10824.

Fages C, Khelil M, Rolland B, Bridoux AM, and Tardy M (1988) Glutamine synthetase: a marker of an astroglial subpopulation in primary cultures of defined brain areas. *Dev Neurosci* **10:**47–56.

Fernando SR and Pertwee RG (1997) Evidence that methyl arachidonyl fluorophosphonate is an irreversible cannabinoid receptor antagonist. *Br J Pharmacol* **121:** 1716–1720.

Furshpan EJ, MacLeish PR, O'Lague PH, and Potter DD (1976) Chemical transmission between rat sympathetic neurons and cardiac myocytes developing in microcultures: evidence for cholinergic, adrenergic, and dual-function neurons. *Proc Natl Acad Sci U S A* **73:**4225–4229.

Gaoni Y and Mechoulam R (1964) Isolation, structure and partial synthesis of an active constituent of hashish. *J Am Chem Soc* **86:**1646–1647.

Gulyas AI, Cravatt BF, Bracey MH, Dinh TP, Piomelli D, Boscia F, and Freund TF (2004) Segregation of two endocannabinoid-hydrolyzing enzymes into pre- and postsynaptic compartments in the rat hippocampus, cerebellum and amygdala. *Eur J Neurosci* **20:**441–458.

Hashimotodani Y, Ohno-Shosaku T, and Kano M (2007) Presynaptic monoacylglycerol lipase activity determines basal endocannabinoid tone and terminates retrograde endocannabinoid signaling in the hippocampus. *J Neurosci* **27:**1211–1219.
Institute of Laboratory Animal Resources (1996) *Guide for the Care and Use of Laboratory Animals*, 7th ed. Institute of Laboratory Animal Resources, Commission on Life Sciences, National Research Council, Washington DC.
Kellogg R, Mackie K, and Straiker A (2009) Cannabinoid CB1 receptor-dependent long-term depression in autaptic excitatory neurons. *J Neurophysiol* **102:**1160–1171.
Kim J and Alger BE (2004) Inhibition of cyclooxygenase-2 potentiates retrograde endocannabinoid effects in hippocampus. *Nat Neurosci* **7:**697–698.
King AR, Duranti A, Tontini A, Rivara S, Rosengarth A, Clapper JR, Astarita G, Geaga JA, Luecke H, Mor M, et al. (2007) URB602 inhibits monoacylglycerol lipase and selectively blocks 2-arachidonoylglycerol degradation in intact brain slices. *Chemistry & biology* **14:**1357–1365.
Koutek B, Prestwich GD, Howlett AC, Chin SA, Salehani D, Akhavan N, and Deutsch DG (1994) Inhibitors of arachidonoyl ethanolamide hydrolysis. *J Biol Chem* **269:**22937–22940.
Kozak KR, Prusakiewicz JJ, and Marnett LJ (2004) Oxidative metabolism of endocannabinoids by COX-2. *Curr Pharm Des* **10:**659–667.
Kozak KR, Rowlinson SW, and Marnett LJ (2000) Oxygenation of the endocannabinoid, 2-arachidonylglycerol, to glyceryl prostaglandins by cyclooxygenase-2. *J Biol Chem* **275:**33744–33749.
Kreitzer AC and Regehr WG (2001a) Cerebellar depolarization-induced suppression of inhibition is mediated by endogenous cannabinoids. *J Neurosci* **21:**RC174.
Kreitzer AC and Regehr WG (2001b) Retrograde inhibition of presynaptic calcium influx by endogenous cannabinoids at excitatory synapses onto Purkinje cells. *Neuron* **29:**717–727.
Levison SW and McCarthy KD (1991) Characterization and partial purification of AIM: a plasma protein that induces rat cerebral type 2 astroglia from bipotential glial progenitors. *J Neurochem* **57:**782–794.
Li W, Blankman JL, and Cravatt BF (2007) A functional proteomic strategy to discover inhibitors for uncharacterized hydrolases. *J Am Chem Soc* **129:**9594–9595.
Lio YC, Reynolds LJ, Balsinde J, and Dennis EA (1996) Irreversible inhibition of Ca(2+)-independent phospholipase A2 by methyl arachidonyl fluorophosphonate. *Biochim Biophys Acta* **1302:**55–60.
Long JZ, Li W, Booker L, Burston JJ, Kinsey SG, Schlosburg JE, Pavón FJ, Serrano AM, Selley DE, Parsons LH, et al. (2009) Selective blockade of 2-arachidonoylglycerol hydrolysis produces cannabinoid behavioral effects. *Nature chemical biology* **5:**37–44.
Makara JK, Mor M, Fegley D, Szabó SI, Kathuria S, Astarita G, Duranti A, Tontini A, Tarzia G, Rivara S, et al. (2005) Selective inhibition of 2-AG hydrolysis enhances endocannabinoid signaling in hippocampus. *Nat Neurosci* **8:**1139–1141.
Matsuda LA, Lolait SJ, Brownstein MJ, Young AC, and Bonner TI (1990) Structure of a cannabinoid receptor and functional expression of the cloned cDNA. *Nature* **346:**561–564.
Melis M, Pistis M, Perra S, Muntoni AL, Pillolla G, and Gessa GL (2004) Endocannabinoids mediate presynaptic inhibition of glutamatergic transmission in rat ventral tegmental area dopamine neurons through activation of CB1 receptors. *J Neurosci* **24:**53–62.
Munro S, Thomas KL, and Abu-Shaar M (1993) Molecular characterization of a peripheral receptor for cannabinoids. *Nature* **365:**61–65.
Norenberg MD and Martinez-Hernandez A (1979) Fine structural localization of glutamine synthetase in astrocytes of rat brain. *Brain Res* **161:**303–310.
Ohno-Shosaku T, Maejima T, and Kano M (2001) Endogenous cannabinoids mediate retrograde signals from depolarized postsynaptic neurons to presynaptic terminals. *Neuron* **29:**729–738.
Saario SM, Palomäki V, Lehtonen M, Nevalainen T, Järvinen T, and Laitinen JT (2006) URB754 has no effect on the hydrolysis or signaling capacity of 2-AG in the rat brain. *Chem Biol* **13:**811–814.
Saario SM, Salo OM, Nevalainen T, Poso A, Laitinen JT, Järvinen T, and Niemi R (2005) Characterization of the sulfhydryl-sensitive site in the enzyme responsible for hydrolysis of 2-arachidonoyl-glycerol in rat cerebellar membranes. *Chem Biol* **12:**649–656.
Shen M and Thayer SA (1998) The cannabinoid agonist Win55,212–2 inhibits calcium channels by receptor-mediated and direct pathways in cultured rat hippocampal neurons. *Brain Res* **783:**77–84.
Stella N, Schweitzer P, and Piomelli D (1997) A second endogenous cannabinoid that modulates long-term potentiation. *Nature* **388:**773–778.
Straiker A and Mackie K (2005) Depolarization-induced suppression of excitation in murine autaptic hippocampal neurones. *J Physiol* **569:**501–517.
Straiker A and Mackie K (2007) Metabotropic suppression of excitation in murine autaptic hippocampal neurons. *J Physiol* **578:**773–785.
Straiker A and Mackie K (2009) Cannabinoid signaling in inhibitory autaptic hippocampal neurons. *Neuroscience* **163:**190–201.
Sullivan JM (1999) Mechanisms of cannabinoid-receptor-mediated inhibition of synaptic transmission in cultured hippocampal pyramidal neurons. *J Neurophysiol* **82:**1286–1294.
Tansey FA, Farooq M, and Cammer W (1991) Glutamine synthetase in oligodendrocytes and astrocytes: new biochemical and immunocytochemical evidence. *J Neurochem* **56:**266–272.
Trettel J and Levine ES (2003) Endocannabinoids mediate rapid retrograde signaling at interneuron right-arrow pyramidal neuron synapses of the neocortex. *J Neurophysiol* **89:**2334–2338.
Wilson RI, Kunos G, and Nicoll RA (2001) Presynaptic specificity of endocannabinoid signaling in the hippocampus. *Neuron* **31:**453–462.
Wilson RI and Nicoll RA (2001) Endogenous cannabinoids mediate retrograde signalling at hippocampal synapses. *Nature* **410:**588–592.
Yanovsky Y, Mades S, and Misgeld U (2003) Retrograde signaling changes the venue of postsynaptic inhibition in rat substantia nigra. *Neuroscience* **122:**317–328.

Address correspondence to: Alex Straiker, Department of Psychological and Brain Sciences, Gill Center for Biomolecular Science, Indiana University, Bloomington, IN 47405. E-mail: straiker@indiana.edu